Assessing the Phenology of Southern Tropical Africa: A Comparison of Hemispherical Photography...

Article *in* IEEE Transactions on Geoscience and Remote Sensing · January 2014

DOI: 10.1109/TGRS.2013.2242081

CITATIONS
8

READS
47

5 authors, including:

Casey M. Ryan
The University of Edinburgh
56 PUBLICATIONS **1,447** CITATIONS
SEE PROFILE

Mathew Williams
The University of Edinburgh
201 PUBLICATIONS **7,492** CITATIONS
SEE PROFILE

Iain Woodhouse
The University of Edinburgh
130 PUBLICATIONS **1,472** CITATIONS
SEE PROFILE

Assessing the Phenology of Southern Tropical Africa: A Comparison of Hemispherical Photography, Scatterometry, and Optical/NIR Remote Sensing

Casey M. Ryan, Mathew Williams, Timothy C. Hill, John Grace, and Iain H. Woodhouse

***Abstract*—The seasonal cycle of tree leaf display in the savannas and woodlands of the seasonally dry tropics is complex, and robust observations are required to illuminate the processes at play. Here, we evaluate three types of data for this purpose, comparing scatterometry (QuikSCAT σ^0) and optical/near-infrared MODIS EVI remotely sensed data against field observations. At a site in Mozambique, the seasonal cycles from both space-borne sensors are in close agreement with each other and with estimates of tree plant area index derived from hemispherical photography ($r > 0.88$). This agreement results in similar estimates of the start of the growing season across different data types (range 13 days). Ku-band scatterometry may therefore be a useful complement to vegetation indices such as EVI for estimating the start of the growing season for trees in tropical woodlands. More broadly, across southern tropical Africa there is close agreement between scatterometry and EVI time series in woody ecosystems with $> 25\%$ tree cover, but in areas of $< 25\%$ tree cover, the two time series diverge and produce markedly different start of season (SoS) dates (difference > 50 days). This is due to increases in σ^0 during the dry season, not matched by increase in EVI. The reasons for these increases are not obvious, but might relate to soil moisture, flowering, fruiting, or grass dynamics. Further observations and modeling of this phenomenon is warranted to understand the causes of these dry season changes in σ^0. Finally, three different definitions of the SoS were examined and found to produce only small differences in estimated dates, across all types of data.**

***Index Terms*—Canopy phenology, land surface phenology (LSP), scatterometry, start of season.**

I. Introduction

THE TIMING of leaf display in tree species determines the duration of major fluxes of water, energy, and carbon between the biosphere and atmosphere [1]–[3]. In the seasonally dry tropics, trees are highly variable in their phenological behavior, ranging from deciduous to briefly deciduous to evergreen [4], [5]. In the tropics, environmental control of leaf emergence is presumed to be related not to temperature (as in temperate and boreal regions), but neither is it simply related to patterns of precipitation and soil moisture [6]–[9].

Improved understanding of tropical tree phenology is contingent on accurate measurements of phenological behavior. Such measurements can be ground based and often involve the recording of an event of interest in the canopy such as bud burst, or the collection of time series data such as carbon fluxes or leaf area index. Ground-based phenological data are, however, very sparse in many regions, particularly in tropical Africa [10]. A complementary approach is to use Earth observation (EO) data to record (bio)physical properties of the Earth surface that relate to phenological patterns of interest. Such data describe the land surface phenology (LSP, [11]) and offer the advantages of regular and global data acquisition, but difficulties remain in linking LSP to ecological measures of canopy phenology [11]–[13].

Optical and near infrared reflectances have been the workhorses of LSP studies to date [11], often combined into an index such as normalized difference vegetation index or enhanced vegetation index (EVI, [14]). However, such data acquisition is not without its difficulties: darkness, atmospheric composition, clouds, and off-nadir viewing angles all reduce the availability of high quality, consistent measures of the land surface. Low- or medium-resolution active microwave remote sensing from scatterometry can also be used as source of LSP data and provides some relief from these constraints [15]–[18]. Scatterometry is however, less widely used in monitoring vegetation phenology, and scatterometry LSP time series have not been widely related to ground-based canopy phenology data [18]. Ku-band scatterometry from the SeaWinds-on-QuikSCAT sensor has been shown to give comparable information to EVI in some vegetation types [16] and to be useful for monitoring tropical grasslands [18], [19]. Ku-band wavelength (2.1 cm) is similar to many leaf lengths, and so a strong interaction between the microwave radiation and the leaves is expected [20] suggesting that these data could be a useful source of information on tree leaf phenology and might provide a useful complement to optical LSP data. However, the two data sources respond to fundamentally different aspects of the land surface: scatterometry data are likely to respond to vegetation structure and moisture contents, as well as being influenced by soil

Manuscript received June 19, 2012; revised November 1, 2012; accepted December 5, 2012. Date of publication February 26, 2013; date of current version November 26, 2013.

C. M. Ryan, M. Williams, J. Grace, and I. H. Woodhouse are with the School of GeoSciences, University of Edinburgh, Edinburgh EH9 3JN, U.K. (e-mail: casey.ryan@ed.ac.uk; mat.williams@ed.ac.uk; jgrace@ed.ac.uk; i.h.woodhouse@ed.ac.uk).

T. C. Hill was with the University of Edinburgh, Edinburgh EH9 3JN, U.K. He is now with the University of St. Andrews, St. Andrews, KY16 9AL, U.K. (e-mail: tch2@st-andrews.ac.uk).

Color versions of one or more of the figures in this paper are available online at http://ieeexplore.ieee.org.

Digital Object Identifier 10.1109/TGRS.2013.2242081

moisture, whereas EVI data will respond to chlorophyll content and the amount of green leaf material.

A further issue in comparing LSP to canopy phenology is the method for extracting dates of phenological events from time series of LSP data [21]–[23]. For instance, a common date of interest is the start of (growing) season date (SoS), the point at which tree leaf expansion starts. This date has been estimated from time series of LSP data in many ways, all of which are heuristic and have only limited relation to the biological event of interest, e.g., SoS is often defined as the point at which the EO quantity reaches half its annual maximum. Such definitions of SoS are often tangential to the canopy processes of interest and the relationship between the two needs to be established empirically. In this paper, we evaluate this relationship between LSP and canopy phenology, and in particular how this relationship depends on both the type of LSP data (optical or scatterometry) and the definition of SoS. This is the first study to investigate the relationship between different SoS definitions derived from ground-based measurements, optical, and microwave EO data.

Our study uses a detailed ground-based data set from a well-studied site in the woodlands of central Mozambique. We complement this with a regional study across all of southern tropical Africa, a region with complex climatology, topography, and vegetation [24].

Key Questions

- How does LSP derived from different EO data types (optical and microwave) compare to ground-based estimates of canopy phenology?
- In which ecosystems of southern tropical Africa are microwave- and optical-derived phenologies congruent and what are the characteristics of areas where the two data sets diverge?
- How similar are SoS dates derived from the different data types, and how is this affected by the specific way in which SoS is identified in the time series data?

II. Methods

Our methods consist of four components: 1) Collection of ground-based plant area index (PAI) data at a site in the woodlands of central Mozambique over 4 years; 2) processing of satellite LSP data at the Mozambique site and for all of southern tropical Africa over 10 years; 3) analysis of the time series data including: cross correlation analysis; estimation of SoS dates based on different definitions; and 4) comparison of the regional EO phenologies to land cover and vegetation maps.

A. Data Collection: Mozambique Site

1) Site Details: Fourteen square one ha permanent sample plots were installed in a range of woodland types in the Nhambita area of Gorongosa District, Sofala province, Mozambique in June 2004 [25]. The plots are spread across an area approximately 20 km by 30 km (centered on S18.979°, E34.176°), adjacent to the Gorongosa National Park. The vegetation on the plots included: 1) dry miombo woodland regrowing after clearance for agriculture; 2) dry miombo degraded by the removal of large stems for charcoal production; 3) relatively undisturbed miombo in the National Park, both fenced and unfenced; and 4) Combretum savanna on more hydromorphic soils [26]. The plots were randomly located along the track and road network in the area and were all $\geq$ 250 m from a road or track. The location of the plots, on the western flank of the Rift Valley, means that they span a range of altitude from 36–300 m, with corresponding changes in drainage and soil type.

2) PAI: We monitored the seasonal cycle of PAI of trees using monthly hemispherical photography [27] for 48 months from June 2004 to May 2008 (inclusive). On each plot, each month, we acquired nine images on a 20 $\times$ 20 m grid. Images were obtained under diffuse light conditions—either at dawn or dusk, or during overcast conditions—and from identical positions with the camera body oriented to the north and the lens rotated to the vertical. We used a Nikon Coolpix 4500 with a FC-E8 fully hemispheric fisheye converter on a leveled tripod at 1.5 m height. For logistical reasons, we were unable to collect photos in seven of the 48 months of this study. A total of 4718 photos were acquired, coded with date and location, and stored in a database (FileMaker Pro, Apple Computer Inc., CA). Each image was visually inspected, and badly exposed or directly illuminated images were discarded (380 images). The images were then analyzed to estimate PAI using the method of [28].

3) Precipitation: Rain gauge data for the Nhambita study area were obtained from three sources: 1) daily rainfall totals from a manual rain gauge at the Gorongosa National Park headquarters at Chitengo, 25 km from the study site (Oct 2000–Nov 2005, provided by ARA CENTRO); 2) half hourly totals of rainfall from an automated weather station (Skye Instruments, U.K.) installed as part of this study adjacent to the Park gauge (Nov 2005–May 2008); 3) a manual gauge operated as part of this project at the center of our study area. Data from 3) were used for a 4 month period (Nov 2007–Feb 2008) when the automatic gauge failed. For a 5 month period (November 2006–March 2007) when all three data sets are available, they show cumulative rainfall of 860, 860, and 878 mm, respectively. As these values are similar, we did not adjust the data from the different sources, and they were combined into one daily resolution time series.

B. EO LSP Data

1) MODIS EVI Data: Nine Moderate Resolution Imaging Spectroradiometer (MODIS) pixels of ground size 0.05° (~5.6 km) cover the 14 plots. EVI data [14] was obtained for these 9 pixels from both MODIS platforms, Terra and Aqua, and were provided as 16-day composites, 8 days out of synchrony with each other. The 0.05° resolution data is, although not the highest resolution available, suitable for extension to the regional scale analyses, and we extracted data for 2000–2010. The 16-day composite product processes daily acquisitions using one of three compositing techniques [14] to minimize problems associated with clouds and off-nadir views.

We discarded all EVI data not flagged as "good" or "marginal" quality in the MODIS QA scheme and linearly interpolated over missing data values. The Terra and Aqua products were interleaved to create a time series of nominal 8 day

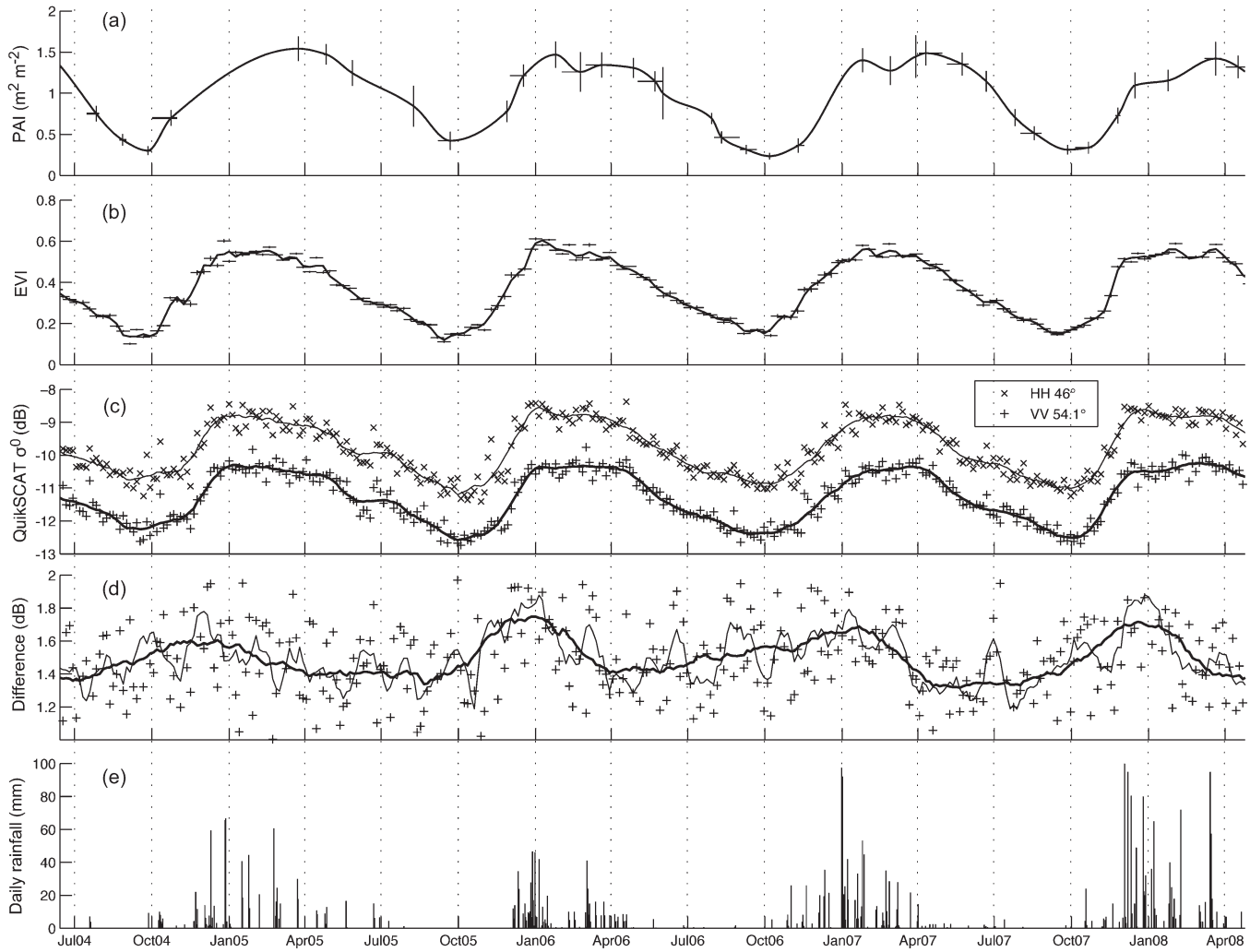

Fig. 1. Phenology of the woodlands of Nhambita, Mozambique. (a) Plant area index of the tree canopy derived from 14 permanent sample plots. Crosses show the full range of dates over which observations were taken on the plots and ± 1 SE of the 14 plots. The line shows a smoothed fit using a cubic spline. (b) MODIS EVI for the nine 0.05° pixels that cover the plots. The crosses show the time span over which each observation is composited and the SE of the nine pixels. (c) QuikSCAT σ^0 for the nine pixels that cover the study area. The smooth lines are the result of a Savitzky-Golay filter with a 21 day window. (d) The difference between HH and VV σ^0. Two smoothed lines are shown, one (thin) with a 21 day window, the other (thick) with a 31 day window. (e) daily rainfall from local rain gauges.

resolution, although the real acquisition dates are a combination of dates from the higher resolution data. A smoothed time series was created using a second-order Savitzky-Golay filter with a window of five data points. This relatively short window minimizes the problem of shifting the time series as an artifact of the filtering.

2) Scatterometry Data: Ku-band normalized radar cross-section (σ^0) measurements from the SeaWinds instrument aboard QuikSCAT were obtained from the NASA Scatterometer Climate Record Pathfinder project [29], [30]. The SeaWinds instrument makes dual polarization measurements of σ^0 at both vertical (VV, 54.1° nominal incidence angle) and horizontal (HH, 46°) polarizations using a conically scanning pencil-beam antenna. The Scatterometer Climate Record Pathfinder project provides enhanced resolution products, increasing the relatively coarse scale (25 km) of the original data using the Scatterometer Image Reconstruction (SIR) algorithm [29], [31], [32]. This method is based on utilizing the frequent overpasses and wide swath to improve spatial resolution at the expense of temporal resolution, assuming no change in land surface properties over 4 days. The 4-day composite "egg" images were used, which have a nominal image pixel resolution of 4.45 km/pixel but an effective resolution of ∼8–10 km in most areas. The images were interpolated to a 0.05° grid (∼5.5 km) using Delaunay triangulation. Significant deviation from the "no change" assumption is expected to occur only during the early part of the onset of the rainy season, where specific rain events will change the surface characteristics (in terms of soil moisture) over a short period of time. The impact will be added uncertainty when using data at the higher resolution. The data smoothing applied within the SIR algorithm is expected to minimize the impact of this issue.

The σ^0 data had a different signal-to-noise ratio and a more consistent magnitude of high-frequency variation, compared to the EVI data. A Savitzky-Golay filter with a 21 data point window removed the high-frequency variations and again did not noticeably "shift" the time series. Raw and smoothed data are shown in Fig. 1. There were no missing σ^0 data.

C. Regional Data Collection

For the regional analysis, we used the EO products described above, acquiring the full data sets for the area bounded by 2° to 26° S and 10° to 41° E. Regional rainfall data from the Tropical Rainfall Measuring Mission (TRMM) were acquired from the NASA Goddard Earth Sciences Data and Information Services Center. We used the 3B42 daily product which uses a combination of infrared and microwave observations scaled to match monthly rain gauge analyses. Data were obtained at 0.25° spatial resolution and linearly interpolated to 0.05°.

The regional phenology data were analyzed by vegetation type based on [24], which is based on pre-satellite era maps and expert interpretation and is thus independent of our EO data. We further analyzed the regional phenology using the 2005 MODIS vegetation continuous fields product (VCF, collection 4, version 3) [33]. The 500 m product was reprojected and interpolated using a bicubic spline to match the 0.05° lat/long grid of the other data sets. We note that the tree cover data are not fully independent of the EVI time series data as some of the same reflectance data are used in the generation of the tree cover product; however, the data used in the tree cover product only represent a small portion of the time series of EVI.

D. Analysis Methods

We developed a set of definitions and related methods to convert time series of data into estimates of SoS. Many definitions and techniques have been used to derive LSP SoS from reflectance data [8], [21], [23], [34]–[36], but with no consensus as to the optimum technique. The challenge is to avoid spuriously classing noise in the signal as SoS, whilst detecting SoS as accurately as possible. Here, we define the SoS as the time point where tree leaf bud break begins. For a given time series of phenology data, p, the SoS must postdate or equal the annual minimum of p, $p_{\min}$, and of course, predate the following annual maximum. Many existing approaches define SoS as the mid point between annual minima and maxima [9]. However, here we are concerned with the *start* of the growing season, not some mid point. Two such definitions were found in the literature; the first [35] is based on fitting logistic functions to phenological transitions, but these functions did not yield useable fits to our data. The second, which did work effectively, utilized a backward-looking moving average (see [23] modified by [8]). We term the resulting SoS date $\mathrm{SoS}_{\mathrm{AS}}$. To complement this definition, we developed two new ones: SoS_{LT} which looks for the start point of the first significant $(\mathrm{P} > 0.05)$ positive linear trend in p, and $\mathrm{SoS}_{\mathrm{ON}}$ which looks for the first three values of p to be significantly (2 SD of the noise) above the minimum. A description of the three definitions is provided in the Appendix. We also refer to p_{10}, which is 10% of the maximum of p for that growing season. This value provides a benchmark for assessing the reliability of SoS dates, and we assume that SoS should fall between $p_{\min}$ and p_{10}.

Estimates of SoS day-of-year are subscripted with the SoS definition (one of $_{\mathrm{AS}}$, $_{\mathrm{LT}}$ or $_{\mathrm{ON}}$ described above) and the source of the data used for the estimate, e.g., $\mathrm{SoS}_{\mathrm{AS,PAI}}$ indicates the SoS date from the backward-looking moving average derived from the PAI data, $\mathrm{SoS}_{\mathrm{AS,EVI}}$ for the SoS defined by the same method from the EVI data and $\mathrm{SoS}_{\mathrm{AS,VV}}$ and $\mathrm{SoS}_{\mathrm{AS,HH}}$ for the scatterometry data in each polarization.

TABLE I
START OF SEASON DAY-OF-YEAR (MEAN ± SD OF 4 YEARS) FOR A SITE IN THE MIOMBO WOODLANDS OF MOZAMBIQUE

Data source	SoS definition		
	LT	AS	ON
PAI	271±6	273±6	
EVI	267±8	283±12	282±10
σ^0_{VV}	277±17	285±17	295±14
σ^0_{HH}	276±19	284±17	293±14

To assess the congruence of the time series of EVI, PAI, σ^0_{HH}, and σ^0_{VV}, correlation coefficients were determined for the relationship of each time series against the other (denoted r). We also used cross correlation analysis to look for evidence of lags between the data series. SoS dates were derived for all the years when data were available and compared between data sources (PAI, EVI, σ^0_{HH} and σ^0_{VV}) and the three SoS definitions (LT, AS, ON).

III. RESULTS

A. Local Observations

Based on the PAI, EVI, and σ^0 data, leaf display on the Nhambita plots had a seasonal cycle with little interannual variability. PAI peaked in February/March and then fell to a minimum in September/October (Fig. 1) rising directly after the minimum in a brevi-deciduous manner. Small rain events were observed after October each year, with the main rains arriving from Oct 17 to Dec 9.

The time series of PAI, σ^0, and EVI showed good agreement [Fig. 1(a)–(c)] with significant correlations between each data source. PAI was best correlated to EVI $(r = 0.94)$, and $\sigma^0_{\mathrm{VV}}(r = 0.90)$ followed by $\sigma^0_{\mathrm{HH}}(r = 0.88)$. The EO time series (EVI and σ^0) were also all well correlated to each other (all $r > 0.95$).

Judged by the cross-correlation coefficients, the seasonal cycle of PAI was shifted earlier that the LSP time series. σ^0_{VV} lagged PAI by 10 days, σ^0_{HH} lagged PAI by 15 days, and EVI lagged PAI by 18 days. These lags should be viewed in the context of the monthly time step of the PAI data. The HH polarization always returned a higher σ^0 than the VV (a difference of around 1.4 to 1.8 dB, which is expected due to the smaller incidence angle of the HH) and the HH:VV ratio varied with the seasonal cycle from 0.84 to 0.88, broadly in synchrony with leaf display.

SoS in Nhambita (Table I), based on PAI data and the LT definition $(\mathrm{SoS}_{\mathrm{LT,PAI}})$, occurred on similar dates each year: 25 Sept 2004, 21 Sept 2005, 6 Oct 2006, and 26 Sept 2007. The range of these dates is well within the 1 month resolution of the time series. It should be noted that in 2005, PAI data are missing near the SoS date. Mean SoS dates using the AS definition occurred 2 days later on average than with the LT definition (27 Sept ±6 vs 29 Sept ±6 days). These SoS dates substantially preceded the point at which the time series reached 10% of its maximum each year ($p_{10,\mathrm{PAI}} = 26$ Oct ±14 days).

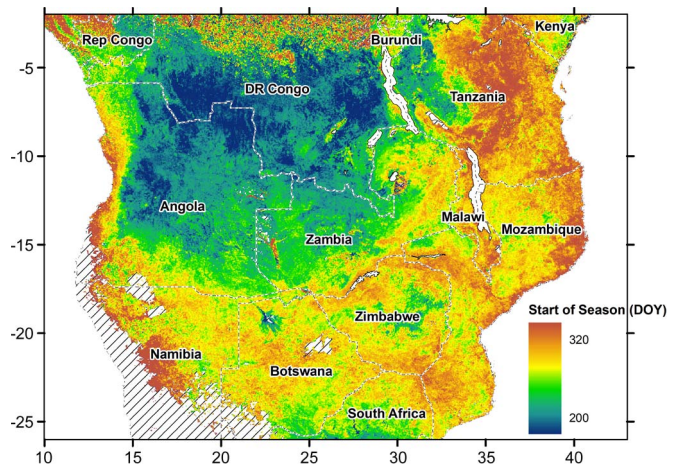

Fig. 2. Day of year of the start of growing season based on EVI data and using the linear trend definition of SoS. Areas where no SoS could be estimated are shown with diagonal lines.

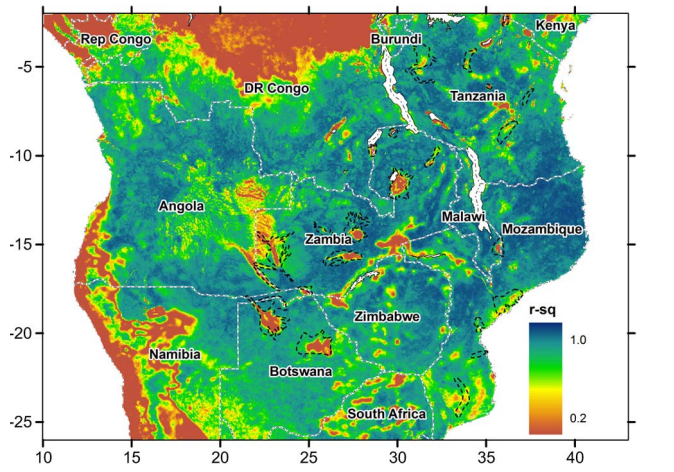

Fig. 3. Map of correlation (r^2) between EVI and scatterometry (σ^0_{HH}) time series. Areas of inundated grassland defined by the WWF eco-regions map [46] are marked with a thick dashed black line.

Mean SoS estimates ranged over 28 days for all definitions and data sources (Table I). Of the definitions, LT was generally the earliest, followed by AS and then ON. The scatterometry-derived SoS were always later than the EVI or PAI SoS dates. The range of SoS dates between definitions was slightly greater than the difference caused by the different data sources, and the relative difference caused by different data sources were consistent across SoS definitions. SoS dates derived from scatterometry were more variable between years than those from EVI, with PAI data giving the most consistent results.

B. Regional Analysis

Looking across our regional study area and using $\mathrm{SoS}_{\mathrm{EVI,AS}}$ as an example, SoS arrived earliest in Angola and the Congo basin, spreading south and then east into Zambia, Botswana, Zimbabwe and Mozambique by day of year (DOY) 275 and arriving last on the east cost of Tanzania and Mozambique (DOY 300–350) (Fig. 2).

The correlation between the two EO data types, EVI and σ^0, varied considerably across the study area but was high for most areas (Fig. 3): 76% of the study area showed $r > 0.8$ and 52% had $r > 0.9$ (r is reported at zero lag). The HH polarized scatterometry data were slightly better correlated to EVI than the VV, but both polarizations showed very similar patterns. For the remainder of the paper, we discuss only the σ^0_{HH} results. Locations with markedly low EVI versus σ^0_{HH} correlation are generally areas with seasonally inundated floodplains of large drainage systems such as the Zambezi, sparsely vegetated areas in the SW, and the equatorial forests of the Congo basin. The highest correlations were found in the woodland land-cover types (Table II) and in areas of intermediate tree cover. The sparsely wooded savannas in the SW had weaker correlations compared to the more tree-dominated systems to the north and east.

The strong correlations between scatterometry and EVI time series did not translate to similar SoS dates in many parts of the study area (Fig. 4). Areas where SoS dates (mean of the three definitions) agreed well included most of the miombo woodlands and areas with moderate woody cover. In contrast,

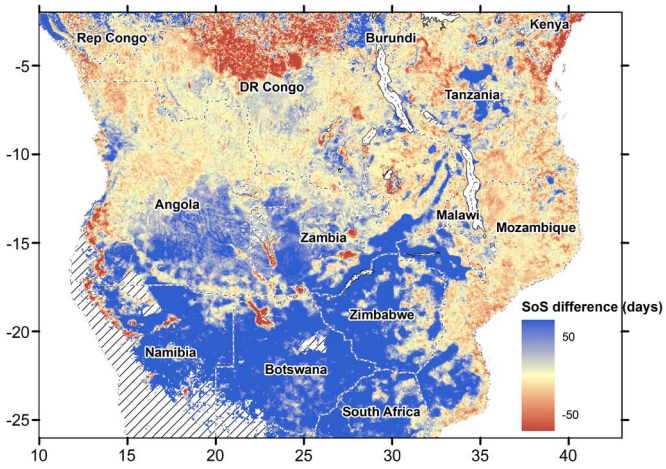

Fig. 4. Difference between SoS dates derived from EVI and scatterometry (σ^0_{HH}). Positive numbers indicate areas where start of season (SoS) dates estimated from scatterometry are earlier than EVI-derived dates. SoS dates are the mean of 10 years and the three definitions of SoS. Areas where no SoS could be estimated are shown with diagonal lines.

SoS dates diverged markedly in the south of the study area, including all of Botswana and most of Zimbabwe and the Zambezi valley. Vegetation types (Table II) with a large difference in mean $\mathrm{SoS}_{\mathrm{EVI}}$ compared to $\mathrm{SoS}_{\mathrm{HH}}$ included Kalahari Acacia wooded grassland (mean difference -57 days [negative indicates $\mathrm{SoS}_{\mathrm{HH}}$ is earlier]), undifferentiated woodland (-30), the transition between the two (-55), and Mopane woodland (-47). Dry miombo (-11) showed better agreement as did wet miombo (-5). No major vegetation types had $\mathrm{SoS}_{\mathrm{HH}}$ later than $\mathrm{SoS}_{\mathrm{EVI}}$. Areas where the SoS differed between data types by > 10 days were restricted to areas with $< 25\%$ tree cover (Fig. 5). In areas with tree cover $> 25\%$, mean $\mathrm{SoS}_{\mathrm{EVI}}$ never differed from $\mathrm{SoS}_{\mathrm{HH}}$ by more than 9 days.

Looking in more detail at the areas where SoS dates diverged markedly, the times series of EO data showed an anomalous pattern (Fig. 6). σ^0 fell to a minimum at the start of the dry season but started increasing up to a month before the EVI and before any rainfall. This feature is widespread in Botswana and Zimbabwe and causes the much earlier $\mathrm{SoS}_{\mathrm{HH}}$ values compared to $\mathrm{SoS}_{\mathrm{EVI}}$.

TABLE II
SUMMARY OF PHENOLOGICAL CHARACTERISTICS OF THE MAJOR VEGETATION TYPES OF SOUTHERN TROPICAL AFRICA

Vegetation type*	Area (% of study area)	Mean Start of Season DOY						Correlation (r) between EVI and σ^0 time series		% tree cover from MODIS VCF
		EVI data			Scatterometry (HH) data					
		LT	AS	ON	LT	AS	ON	VV-pol	HH-pol	
Wetter Zambezian miombo woodland	20%	240	248	249	233	237	249	0.91	0.91	35
Drier Zambezian miombo woodland	11%	278	279	282	259	263	275	0.91	0.91	24
Mosaic of lowland rain forest & secondary grassland	9%	229	237	236	228	235	244	0.69	0.73	36
Colophospermum mopane woodland & scrub woodland	8%	285	283	289	226	235	242	0.78	0.79	12
Undifferentiated woodland	6%	273	273	279	232	240	252	0.86	0.86	19
Kalahari Acacia wooded grassland & deciduous bushland	5%	276	271	279	204	212	222	0.77	0.80	2
East African coastal mosaic	5%	293	297	295	296	304	311	0.89	0.90	28
Transition from undifferentiated woodland to Acacia deciduous bushland & wooded grassland.	5%	278	275	283	212	216	227	0.78	0.81	5
Guineo-Congolian rain forest: drier types	4%	246	258	254	258	264	274	0.31	0.30	51
Mosaic of dry deciduous forest & secondary grassland	4%	264	268	272	226	228	244	0.89	0.90	15

The ten most extensive vegetation types are presented, which occupy 76% of the land area of the study region.
*Vegetation types from ref 24

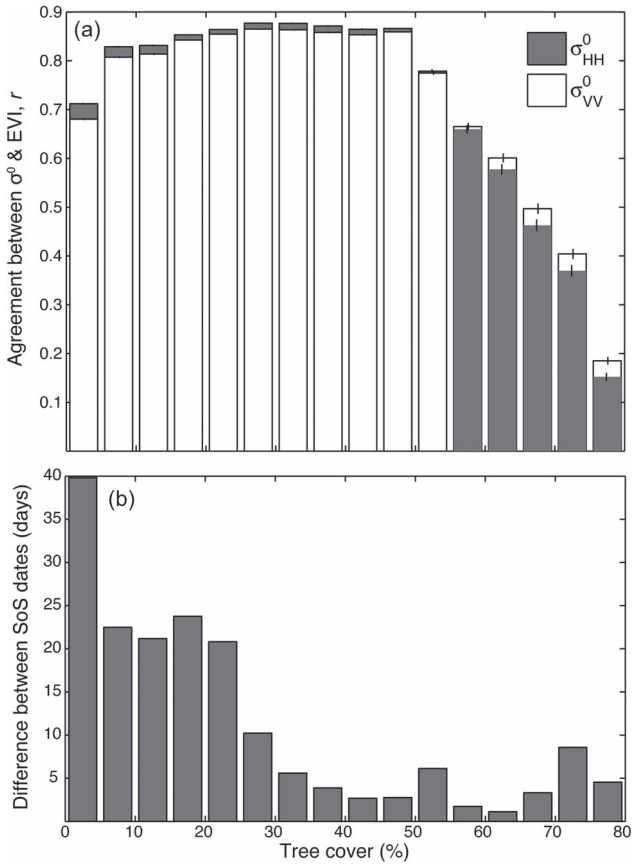

Fig. 5. (a) The correlation (r) between EVI and scatterometry time series as a function of tree cover. (b) The difference in SoS estimates between the two data sources as a function of tree cover.

At the level of vegetation types, the three SoS definitions produce mean SoS dates that diverged by 5–12 days when using EVI data and 14–23 days using the scatterometry data (considering the 10 largest vegetation types). In the more wooded, northern part of the study area, the variability between SoS definitions exceeded the variability between data sources. However, in the southern, sparse savanna areas, the previously noted large variation between EVI- and σ^0-derived SoS dates greatly exceeded the variation between SoS definitions. The three SoS definitions produced more variable results using σ^0 compared to EVI.

The SoS dates fell within the range $p_{\min} < \text{SoS} < p_{10}$ in $> 83\%$ of pixel-years (Table III). No SoS dates were recorded prior to $p_{\min}$ for any SoS definition or data type. However, the ability to detect SoS prior to p_{10} varied considerably between definition and data type. Notably, the LT definition when used with EVI data, and the ON definition when used with scatterometry data failed to detect SoS prior to p_{10} in 11% and 17% of pixel-years (Table III). The AS definition performed best, in that it reliably detected SoS after $p_{\min}$ and before p_{10}, with both data sources.

IV. DISCUSSION

- *How does LSP derived from different EO data types compare to ground-based estimates of canopy phenology?*

Our results from a woodland site in Mozambique show that Ku-band scatterometry and EVI data record a LSP that is closely linked to the canopy phenology recorded by monthly hemispherical photos. SoS dates based on scatterometry data were on average 5–11 days later than those derived from hemispherical photos, depending on the definition of SoS, which, given the monthly resolution of the ground data, suggests no substantive difference. The scatterometry LSP was also very similar to the EVI LSP, both in terms of SoS dates (2–11 days later, depending on SoS definition) and the correlation between time series $(r > 0.94)$.

The close agreement between σ^0 and EVI is expected to be due to several processes [18], including increased soil moisture and green vegetation in the wet season. The green vegetation includes both grass and tree canopy elements and is important due to its higher dielectric constant compared to dry vegetation (therefore increasing volume scattering), and the seasonal dynamics of leaf growth and die-back (which influence both volume scattering and EVI). Changing chlorophyll content will also influence EVI, but not scattering. Soil moisture is the trigger of grass growth, which leads to greater leaf display (and hence EVI), and also increases surface scattering, which increases σ^0 [15], [37].

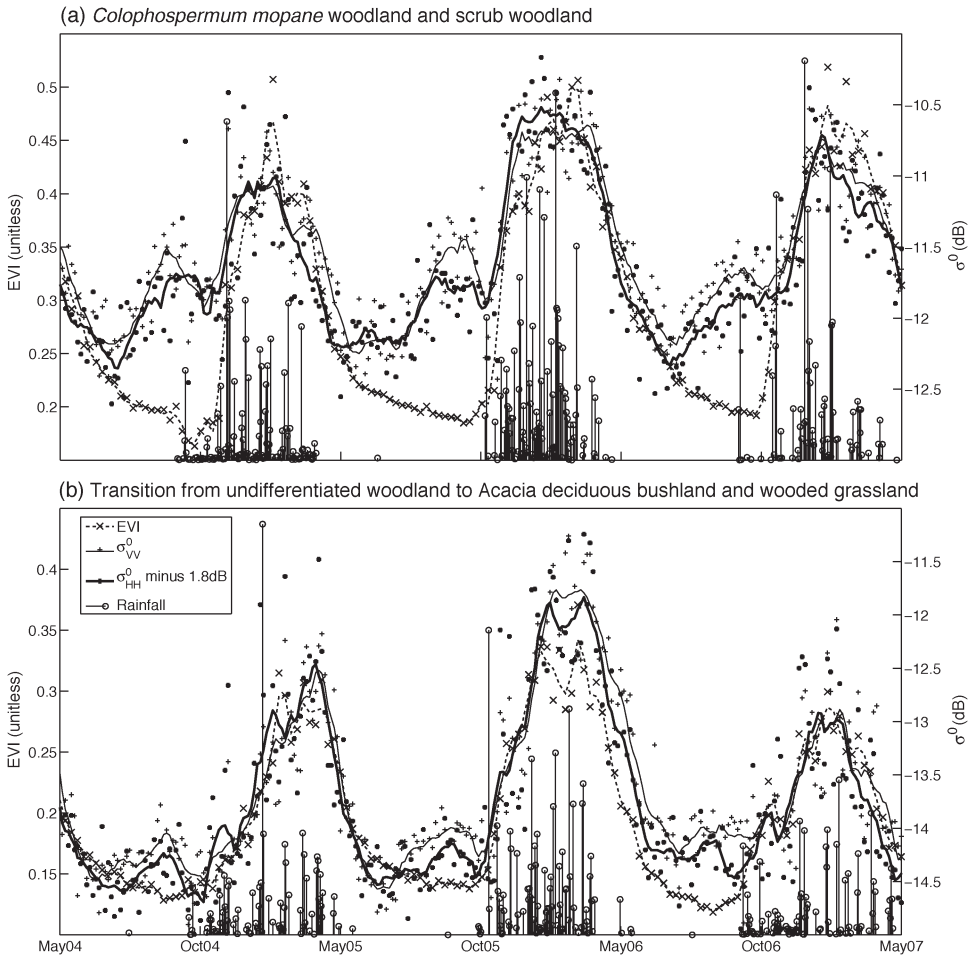

Fig. 6. Time series of EVI and σ^0 for two example locations in sparsely wooded southern Africa. Note the excursion of σ^0 in the late dry season, while EVI is declining and prior to rainfall.

TABLE III
PERCENTAGE OF PIXEL-YEARS WHEN START OF SEASON (SoS) WAS DETECTED PRIOR TO THE TIME SERIES REACHING 10% OF ITS YEARLY MAXIMUM

Data source	SoS definition		
	LT	AS	ON
EVI	11%	5%	1%
σ^0_{HH}	5%	2%	20%
σ^0_{VV}	4%	2%	17%

To our knowledge, no previous studies have compared ground-based tree canopy observations to scatterometry LSP in mixed tree-grass ecosystems. However, at several grassland sites in South America, Hardin and Jackson [18] concluded that changes in σ^0_{HH} and σ^0_{VV} were largely a function of grass biomass or LAI and [19] showed that interannual variability in grass biomass in the USA was related to variability in Ku-band scatterometry. As the Mozambique site has a substantial grass understory [38], grass dynamics are likely contributing to seasonal variations in σ^0 in our study. However, prior to the commencement of the rains, increases in σ^0, EVI, and PAI are observed (Fig. 1). Grass biomass cannot develop before the start of the rainy season [8], [39], [40], but, in contrast, tree leaf expansion can start weeks or months before the rains [5], [8], [9], [40]–[44]. Changes in σ^0 of $\sim$2 dB are observed prior to the onset of the rainy season, suggesting that, in wooded areas, tree canopy phenology drives most of the change in σ^0, a conclusion that is supported by modeling studies [20]. These observations, coupled with the close correlation between PAI (which records only tree phenology, not grass) and σ^0 time series suggest that σ^0 is responding to the development of the tree canopy, perhaps with a further contribution from the grass. Ku-band scatterometry may therefore be useful in determining the start of the growing season for trees in miombo woodland ecosystems.

Reference [18] found that σ^0_{HH} was more sensitive to soil moisture than σ^0_{VV}, resulting in a relationship between the difference, $\sigma^0_{HH} - \sigma^0_{VV}$, and rainfall/soil moisture. We have not standardized the two polarizations to a similar incidence angle, but still see a seasonal variation in the difference that is linked to the pattern of dry and wet seasons, with particularly high values in very intense rainy seasons (2005 and 2007, Fig. 1). However, the magnitude of this variation is small ($\sim$0.2 dB), and variations are observed outwith the rainy season (e.g., Aug. 05, Aug. 07 in Fig. 1).

- *In which ecosystems of southern tropical Africa are microwave and optical-derived phenologies congruent and what are the characteristics of areas where the two data types diverge?*

In line with the findings at the Mozambique site, the scatterometry and EVI data were very well correlated ($r^2 > 0.8$), and produced similar SoS dates, across the miombo woodlands and in regions with $> 25\%$ tree cover. Previous studies have

observed a close link ($r^2 > 0.57$) between MODIS-estimated LAI and σ^0 in some deciduous broadleaf forests in North America, savannas in Benin and Sudan, shrublands in Botswana, and grasslands in N America [16]. We find similar or stronger correlations between EVI and σ^0 in much of southern tropical Africa, including all woodlands, dry forests, sparse savannas and grasslands. Areas where EVI and σ^0 are not significantly correlated included seasonally inundated grasslands and areas with little seasonality (deserts and rain forests). However, in the areas that do exhibit a strong correlation, it is clear that r provides only a crude measure of the similarity of the LSP signals and when SoS dates were extracted, a much more complicated picture emerges.

First, even in areas with very high correlation ($r > 0.91$), scatterometry-derived SoS was often earlier than EVI-derived SoS: by one week in wet miombo and two weeks in dry miombo (Table III). This may reflect the fact that new miombo leaves are not normally green, and new leaves increase in chlorophyll content for up to several weeks after bud burst [45]. Thus, the EVI may be lower for a given leaf area than later in the season. The structural and moisture-related information provided by the scatterometry may thus be decoupled from the biochemical information in the EVI data. However, it may also be that the signal-to-noise ratio and temporal resolution of the σ^0 data are better suited to earlier detection of SoS. In particular, the more frequent observations of σ^0 make the linear trend method more powerful and may enable significant trends to be detected earlier compared to the quasi 8-day intervals between the MODIS products used here.

Second, the more moderate strength of correlation ($0.65 < r < 0.88$) in areas of sparse savanna (tree cover $< 25\%$) in the south of the study area (e.g., Mopane, Acacia savanna, and transition woodlands) belies major discrepancies in LSP during the dry season and the start of the growing season (Fig. 6). These discrepancies result in very large (20–47 days) differences in SoS dates derived from the two sources of LSP data (Fig. 4). The divergence of σ^0 and EVI in areas of sparse woody cover is interesting, and we now speculate on what could cause the observed transient increase in σ^0 prior to the rains (Fig. 6). Increases in soil moisture can probably be ruled out as no rainfall is recorded during the divergence event (and, although TRMM data may miss small rain events, we have found that in Nhambita, TRMM overestimates early season rainfall compared to ground observations, data not shown). However, as the soil dries out, the increased depth of penetration of the radar energy may allow it to interact with previously "hidden" features, such as roots and impermeable pans, which may cause an increase in backscatter via surface scattering. Changes to the soil surface, perhaps due to cracking or fire might play a role, but it is difficult to envisage how these effects could be transient within the dry season. The senescence, structural changes, and changing moisture content of the substantial grass layer in these systems may well play a strong role in altering σ^0 (see above) and deserves further study. It is also possible that dry season fruiting or flowering in the tree canopy could increase σ^0 in the transient manner observed, although whether the magnitude of this effect would correspond to the $\sim$0.5 dB changes observed is questionable. Until this issue is understood, scatterometry-derived LSP cannot be easily related to canopy phenology or other ecological phenomena with confidence in savannas with $< 25\%$ tree cover.

- *How similar are SoS dates derived from the different data types, and how is this affected by the definition of SoS?*

The three SoS definitions produced more variable results using σ^0 compared to EVI. The range between the three SoS definitions was between 1 and 9 days when using EVI data and 15–19 days using the scatterometry data (considering the ten most extensive vegetation types). In the northern part of the study area in the woodlands, the variability between SoS definitions exceeded the variability between data sources. However, in the southern, sparse savanna areas, the previously noted large variation between EVI and σ^0-derived SoS dates greatly exceeded the variation between SoS definitions.

None of the SoS definitions produced SoS dates prior to $p_{\min}$, but their ability to detect SoS before 10% of the season's maximum (p_{10}) varied both by definitions and data sources (Table III). The LT definition, when used with EVI data, failed to detect SoS before p_{10} in 11% of pixel-years, whereas when used with scatterometry data, it only failed in this regard 5% of the time, probably due to the power of more frequent observations. Conversely, the ON definition failed to detect SoS prior to p_{10} in 17–20$\%$ of pixel-years when used with the scatterometry data, but this was reduced to 1% when used with EVI data. This can probably be attributed to the poorer signal-to-noise ratio of the scatterometry data. The AS method was successful in detecting SoS prior to p_{10} in $> 95\%$ of pixel-years, regardless of data type, and is thus the most suitable for use with both data types, whereas the other methods were less useful with one or other of the data types. The AS method also produced intermediate SoS dates, later than LT but prior to ON.

V. Conclusion

At a woodland site in central Mozambique, ground-based PAI measurements recorded a seasonal cycle of leaf display similar to that observed from scatterometry and optical remote sensing. Correlations between the data sources were strong ($r > 0.94$), and SoS dates extracted from the time series were similar (mean difference < 11 days).

At a regional scale, the good agreement between QuikSCAT σ^0 and MODIS EVI was found to extend across the woodlands of southern tropical Africa. In areas with tree cover $> 25\%$, SoS dates estimated with EVI and scatterometry data never differed by > 9 days, suggesting that scatterometry data and EVI are both useful tools for assessing the LSP in African woodland ecosystems.

In more sparsely wooded ecosystems ($< 25\%$ tree cover) such as the Acacia woodlands and Mopane, the σ^0 and EVI time series diverged, with increases in σ^0 in the dry season, months prior to EVI increases or TRMM-recorded rainfall. This anomalous σ^0 increase resulted in much earlier SoS dates being recorded from scatterometry data in comparison to EVI data (> 30 days). Possible reasons for this difference include variations in soil moisture or soil roughness, the occurrence of tree flowering and fruiting, or grass dynamics. Further investigation using ground-based observations and process-based modeling

is warranted to fully understand the causes of the dry season changes in σ^0.

Three different definitions of the SoS produced only modest differences in estimated SoS dates (< 19 days) and produced similar results with both EVI and σ^0 data. A backwards-looking running average method worked best with both σ^0 and EVI data, in that it most often produced SoS dates between the minimum and 10% of each growing season's maximum value of the time series.

APPENDIX

A. Definitions of SoS

All data were analyzed on a per-pixel basis and in separate year-long sections starting from May 1. Each time series was normalized to a range of 0–1 to avoid the influence of the amplitude of the time series in different ecosystems. Both raw and smoothed data (described in the main text) were used. $p_{\min}$ and p_{10} were estimated from the smoothed time series. For robustness, p_{10} was defined as 10% of the 95% percentile of the data for that year.

1) Backwards Looking Running Average (SoS_{AS}): Archibald and Scholes [8] defined the SoS as occurring at measurement i, when

$$p_i > \overline{p_{i-1\ldots i-4}} \tag{1}$$

where p_i is the EO quantity for measurement at time i and $\overline{p_{i-1\ldots i-4}}$ is the mean of the EO quantity of the past four observations.

2) Linear Trend (SoS_{LT}): The LT definition looks for the data point from which there is a significant, positive slope to the following values of p over two time periods. It fits (using linear least squares) two lines, starting at time i and using all data points for the following t_{short} and t_{long} periods (default values 30 and 60 days, respectively). The slopes, s_{short} and s_{long}, of the lines and the probabilities (P_{short} and P_{long}) of obtaining a correlation as large as the observed value by random chance were estimated using the *polyfit* and *corrcoef* functions of Matlab. SoS_{LT} is indicated by all of the following being true: $s_{\text{short}} > 0, s_{\text{long}} > 0, P_{\text{short}} < P_{\text{crit}}, P_{\text{long}} < P_{\text{crit}}$. Where the default value of P_{crit} is 0.05. In addition, an extra constraint was added to ensure that local minima were avoided. Thus, the following must also be true: $p_i < p_{i+1} < p_{i+2}$.

3) Out of the Noise (SoS_{ON}): This method estimates the noise (N) in the signal as the difference between the smoothed data (p) and the observed raw data (p^*). It then defines SoS as the first point after $p_{\min}$ when m consecutive values (default $m = 3$) of p exceed $p_{\min} + N$. SoS_{ON} occurs at time i, when all of the following are true:

$$\begin{aligned} &p^*_{\text{i}} > p_{\min} + N \\ &p^*_{\text{i}+1} > p_{\min} + N \\ &\ldots \\ &p^*_{\text{i}+_m} > p_{\min} + N \end{aligned}$$

where, $N = 1.98 \cdot \sqrt{(\Sigma([p_i - p^*_i] - \overline{[p - p^*]})^2)/(n-1)}$ and n is the number of observations in the annual time series of raw data and smoothed data.

ACKNOWLEDGMENT

The authors gratefully acknowledge the NASA Scatterometer Climate Record Pathfinder project (www.scp.byu.edu), which provided the resolution-enhanced SeaWinds backscatter data. Thanks to T. Quaife (NCEO and University of Reading), R. Clement, S. Bertin, and I. Cameron (University of Edinburgh) for useful discussions. Envirotrade Ltd and the Nhambita community made the fieldwork possible. Special thanks to J. Pennie and G. Goss. Two anonymous reviewers provided helpful and interesting comments.

REFERENCES

[1] T. N. Chase, R. A. Pielke, T. G. F. Kittel, R. Nemani, and S. W. Running, "Sensitivity of a general circulation model to global changes in leaf area index," *J. Geophys. Res.*, vol. 101, no. D3, pp. 7393–7408, Jan. 1996.

[2] D. D. Baldocchi, T. A. Black, P. S. Curtis, E. Falge, J. D. Fuentes, A. Granier, L. Gu, A. Knohl, K. Pilegaard, H. P. Schmid, R. Valentini, K. Wilson, S. Wofsy, L. Xu, and S. Yamamoto, "Predicting the onset of net carbon uptake by deciduous forests with soil temperature and climate data: A synthesis of FLUXNET data," *Int. J. Biometeorol.*, vol. 49, no. 6, pp. 377–387, Jul. 2005.

[3] P. B. Reich, "Phenology of tropical forests: Patterns, causes, and consequences," *Can. J. Bot.*, vol. 73, no. 2, pp. 164–174, Feb. 1995.

[4] R. J. Williams, B. A. Myers, W. J. Muller, G. A. Duff, and D. Eamus, "Leaf phenology of woody species in a North Australian tropical savanna," *Ecology*, vol. 78, no. 8, pp. 2542–2558, Dec. 1997.

[5] S. de Bie, P. Ketner, M. Paasse, and C. Geerling, "Woody plant phenology in the West Africa savanna," *J. Biogeogr.*, vol. 25, no. 5, pp. 883–900, Sep. 1998.

[6] B. A. Myers, R. J. Williams, I. Fordyce, G. A. Duff, and D. Eamus, "Does irrigation affect leaf phenology in deciduous and evergreen trees of the savannas of northern Australia?" *Austral. Ecol.*, vol. 23, no. 4, pp. 329–339, Aug. 1998.

[7] R. Borchert, G. Rivera, and W. Hagnauer, "Modification of vegetative phenology in a tropical semi-deciduous forest by abnormal drought and rain," *Biotropica*, vol. 34, no. 1, pp. 27–39, Mar. 2002.

[8] S. Archibald and R. J. Scholes, "Leaf green-up in a semi-arid African savanna-separating tree and grass responses to environmental cues," *J. Veg. Sci.*, vol. 18, no. 4, pp. 583–594, Aug. 2007.

[9] S. I. Higgins, M. D. Delgado-Cartay, E. C. February, and H. J. Combrink, "Is there a temporal niche separation in the leaf phenology of savanna trees and grasses?" *J. Biogeogr.*, vol. 38, no. 11, pp. 2165–2175, Nov. 2011.

[10] M. D. Schwartz, *Phenology: An Integrative Environmental Science*. Boston, MA, USA: Kluwer, 2003.

[11] L. Liang and M. Schwartz, "Landscape phenology: An integrative approach to seasonal vegetation dynamics," *Landscape Ecol.*, vol. 24, no. 4, pp. 465–472, Apr. 2009.

[12] S. Studer, R. Stockli, C. Appenzeller, and P. L. Vidale, "A comparative study of satellite and ground-based phenology," *Int. J. Biometeorol.*, vol. 51, no. 5, pp. 405–414, May 2007.

[13] D. Doktor, A. Bondeau, D. Koslowski, and F.-W. Badeck, "Influence of heterogeneous landscapes on computed green-up dates based on daily AVHRR NDVI observations," *Remote Sens. Environ.*, vol. 113, no. 12, pp. 2618–2632, Dec. 2009.

[14] A. Huete, K. Didan, T. Miura, E. P. Rodriguez, X. Gao, and L. G. Ferreira, "Overview of the radiometric and biophysical performance of the MODIS vegetation indices," *Remote Sens. Environ.*, vol. 83, no. 1/2, pp. 195–213, Nov. 2002.

[15] I. H. Woodhouse and D. H. Hoekman, "Determining land-surface parameters from the ERS wind scatterometer," *IEEE Trans. Geosci. Remote Sens.*, vol. 38, no. 1, pp. 126–140, Jan. 2000.

[16] S. Frolking, T. Milliman, K. McDonald, J. Kimball, M. Zhao, and M. Fahnestock, "Evaluation of the seawinds scatterometer for regional monitoring of vegetation phenology," *J. Geophys. Res.*, vol. 111, no. D17, p. D17302, Sep. 2006.

[17] W. Wagner, G. Lemoine, M. Borgeaud, and H. Rott, "A study of vegetation cover effects on ERS scatterometer data," *IEEE Trans. Geosci. Remote Sens.*, vol. 37, no. 2, pp. 938–948, Mar. 1999.

[18] P. J. Hardin and M. W. Jackson, "Investigating seawinds terrestrial backscatter: Equatorial savannas of South America," *Photogramm. Eng. Remote Sens.*, vol. 69, no. 11, pp. 1243–1254, Nov. 2003.

[19] S. Frolking, M. Fahnestock, T. Milliman, K. McDonald, and J. Kimball, "Interannual variability in North American grassland biomass/productivity detected by SeaWinds scatterometer backscatter," *Geophys. Res. Lett.*, vol. 32, no. 21, p. L21409, Nov. 2005.

[20] F. T. Ulaby, C. T. Allen, G. Eger Iii, and E. Kanemasu, "Relating the microwave backscattering coefficient to leaf area index," *Remote Sens. Environ.*, vol. 14, no. 1–3, pp. 113–133, Jan. 1984.

[21] M. A. White, K. M. De Beurs, K. Didan, D. W. Inouye, A. D. Richardson, O. P. Jensen, J. O'Keefe, G. Zhang, R. R. Nemani, W. J. D. Van Leeuwen, J. F. Brown, A. De Wit, M. Schaepman, X. Lin, M. Dettinger, A. S. Bailey, J. Kimball, M. D. Schwartz, D. D. Baldocchi, J. T. Lee, and W. K. Lauenroth, "Intercomparison, interpretation, and assessment of spring phenology in North America estimated from remote sensing for 1982–2006," *Global Change Biol.*, vol. 15, no. 10, pp. 2335–2359, Oct. 2009.

[22] M. D. Schwartz and J. M. Hanes, "Intercomparing multiple measures of the onset of spring in eastern North America," *Int. J. Climatol.*, vol. 30, no. 11, pp. 1614–1626, Sep. 2010.

[23] B. C. Reed, J. F. Brown, D. VanderZee, T. R. Loveland, J. W. Merchant, and D. O. Ohlen, "Measuring phenological variability from satellite imagery," *J. Veg. Sci.*, vol. 5, no. 5, pp. 703–714, Nov. 1994.

[24] F. White, *The Vegetation of Africa: A Descriptive Memoir to Accompany the Unesco/AETFAT/UNSO Vegetation Map of Africa*. Paris, France: Unesco, 1983.

[25] C. M. Ryan, M. Williams, and J. Grace, "Above- and belowground carbon stocks in a Miombo woodland landscape of Mozambique," *Biotropica*, vol. 43, no. 4, pp. 423–432, Jul. 2011.

[26] C. M. Ryan, T. Hill, E. Woollen, C. Ghee, E. Mitchard, G. Cassells, J. Grace, I. H. Woodhouse, and M. Williams, "Quantifying small-scale deforestation and forest degradation in African woodlands using radar imagery," *Global Change Biol.*, vol. 18, no. 1, pp. 243–257, Jan. 2012.

[27] D. O. Fuller, "Canopy phenology of some mopane and miombo woodlands in eastern Zambia," *Global Ecol. Biogeogr.*, vol. 8, no. 3/4, pp. 199–209, May–Jul. 1999.

[28] C. M. Ryan and M. Williams, "How does fire intensity and frequency affect miombo woodland tree populations and biomass?" *Ecol. Appl.*, vol. 21, no. 1, pp. 48–60, Jan. 2011.

[29] D. G. Long, P. J. Hardin, and P. T. Whiting, "Resolution enhancement of spaceborne scatterometer data," *IEEE Trans. Geosci. Remote Sens.*, vol. 31, no. 3, pp. 700–715, May 1993.

[30] D. G. Long, "Standard BYU QuikSCAT and Seawinds Land/Ice Image Products," Microw. Earth Remote Sens. Lab., Brigham Young Univ., Provo, UT, USA, 2010. [Online]. Available: http://www.scp.byu.edu/docs/pdf/QscatReport6.pdf

[31] D. S. Early and D. G. Long, "Image reconstruction and enhanced resolution imaging from irregular samples," *IEEE Trans. Geosci. Remote Sens.*, vol. 39, no. 2, pp. 291–302, Feb. 2001.

[32] M. W. Spencer, C. Wu, and D. G. Long, "Improved resolution backscatter measurements with the SeaWinds pencil-beam scatterometer," *IEEE Trans. Geosci. Remote Sens.*, vol. 38, no. 1, pp. 89–104, Jan. 2000.

[33] M. C. Hansen, R. S. DeFries, J. R. G. Townshend, M. Carroll, C. Dimiceli, and R. A. Sohlberg, "Global percent tree cover at a spatial resolution of 500 meters: First results of the MODIS vegetation continuous fields algorithm," *Earth Interact.*, vol. 7, no. 10, pp. 1–15, Oct. 2003.

[34] A. Bachoo and S. Archibald, "Influence of using date-specific values when extracting phenological metrics from 8-day composite NDVI data," in *Proc. Int. Workshop Anal. MultiTemp Remote Sens. Image*, 2007, pp. 1–4.

[35] X. Zhang, M. A. Friedl, C. B. Schaaf, A. H. Strahler, J. C. F. Hodges, F. Gao, B. C. Reed, and A. Huete, "Monitoring vegetation phenology using MODIS," *Remote Sens. Environ.*, vol. 84, no. 3, pp. 471–475, Mar. 2003.

[36] S. Kang, S. W. Running, J. H. Lim, M. Zhao, C. R. Park, and R. Loehman, "A regional phenology model for detecting onset of greenness in temperate mixed forests, Korea: An application of MODIS leaf area index," *Remote Sens. Environ.*, vol. 86, no. 2, pp. 232–242, Jul. 2003.

[37] S. Frolking, T. Milliman, M. Palace, D. Wisser, R. Lammers, and M. Fahnestock, "Tropical forest backscatter anomaly evident in SeaWinds scatterometer morning overpass data during 2005 drought in Amazonia," *Remote Sens. Environ.*, vol. 115, no. 3, pp. 897–907, Mar. 2011.

[38] C. M. Ryan, "Carbon Cycling, Fire and Phenology in a Tropical Savanna Woodland in Nhambita, Mozambique," Ph.D. dissertation, School of Geosci., Univ. of Edinburgh, Edinburgh, U.K., 2009.

[39] W. A. Hoffmann, E. R. da Silva, G. C. Machado, S. J. Bucci, F. G. Scholz, G. Goldstein, and F. C. Meinzer, "Seasonal leaf dynamics across a tree density gradient in a Brazilian savanna," *Oecologia*, vol. 145, no. 2, pp. 307–316, Sep. 2005.

[40] E. N. Chidumayo, "Climate and phenology of savanna vegetation in southern Africa," *J. Veg. Sci.*, vol. 12, no. 3, pp. 347–354, Jun. 2001.

[41] J. L. Devineau, "Seasonal rhythms and phenological plasticity of savanna woody species in a fallow farming system (south-west Burkina Faso)," *J. Trop. Ecol.*, vol. 15, no. 4, pp. 497–513, Jul. 1999.

[42] G. Simioni, J. Gignoux, X. Le Roux, R. Appe, and D. Benest, "Spatial and temporal variations in leaf area index, specific leaf area and leaf nitrogen of two co-occurring savanna tree species," *Tree Physiol.*, vol. 24, no. 2, pp. 205–216, Feb. 2004.

[43] F. C. Do, V. A. Goudiaby, O. Gimenez, A. L. Diagne, M. Diouf, A. Rocheteau, and L. E. Akpo, "Environmental influence on canopy phenology in the dry tropics," *Forest Ecol. Manage.*, vol. 215, no. 1–3, pp. 319–328, Aug. 2005.

[44] P. Frost, "The ecology of Miombo woodlands," in *The Miombo in Transition: Woodlands and Welfare in Africa*, B. M. Campbell, Ed. Bogor, Indonesia: Center for International Forestry Research, 1996, pp. 11–55.

[45] J. S. Choinski and J. M. Johnson, "Changes in photosynthesis and water status of developing leaves of *Brachystegia-Spiciformis* benth," *Tree Physiol.*, vol. 13, no. 1, pp. 17–27, Jul. 1993.

[46] D. M. Olson, E. Dinerstein, E. D. Wikramanayake, N. D. Burgess, G. V. N. Powell, E. C. Underwood, J. A. D'Amico, I. Itoua, H. E. Strand, J. C. Morrison, C. J. Loucks, T. F. Allnutt, T. H. Ricketts, Y. Kura, J. F. Lamoreux, W. W. Wettengel, P. Hedao, and K. R. Kassem, "Terrestrial ecoregions of the world: A new map of life on earth," *BioScience*, vol. 51, no. 11, pp. 933–938, Nov. 2001.

Authors' photographs and biographies not available at the time of publication.